Conformal Beam-steering Antenna Controlled by a Raspberry Pi for Sustained High Throughput Applications

Arpan Pal, *Member, IEEE*, Amit Mehta, *Senior Member, IEEE*, Hasanga Goonesinghe, Dariush Mirshekar-Syahkal, *Fellow IEEE* and Hisamatsu Nakano, *Life Fellow, IEEE*

***Abstract*— A complete autonomous system consisting of a beam steerable Hemispherical Square Loop Antenna (HSLA) controlled by a Raspberry Pi is presented for optimizing the throughput in a scattered and a poor Signal to Noise Ratio (SNR) environment. A total of four different indoor communication configurations at various distances were analyzed in presence of interferences. In three configurations HSLA performance was also compared to that of a standard monopole antenna link. It was found HSLA can offer up to 1450 % higher throughput and can withstand much higher interference levels before the system breaks. In terms of quality this means sustaining compressed HD communications. In effect, it improves the system throughput for the test 2.4 GHz (802.11b/g/n) WiFi band. The uniqueness about the system is that it only uses single antenna for both sensing and communication. The algorithm works at application layer that controls the RF switch and antenna patterns at physical layer. Thus, the entire middle protocol layers are untouched. The system can easily be retrofitted to existing non-adaptive communication systems.**

***Index Terms*—Adaptive algorithm, beam steering, high definition video, impedance matching, raspberry Pi, received signal strength indicator, square loop antenna, throughput.**

I. Introduction

With emerging Fifth generation (5G) mobile communication systems the growing demand for high-throughput wireless communications with ubiquitous coverage is enabling arrival of the new antenna technology. A special aspect of future high-speed internet access has to be on the high-quality video transmissions. Over the next three years 2/3 of the wireless traffic will be video [1]-[2], such as High Definition (HD) video conferencing [3], video on demand, MobiTv [4], electronic classroom [5] and WiFi telecast in smart homes [6]. With the new extended bandwidth allocation in 5G a multi-gigabit / sec data speed will be realizable [7]-[8]. However, those speeds will only work in areas with a high SNR (Signal to Noise Ratio). In situation of a device operating in a weak SNR environment; e.g. away from the base stations or in a rich multipath or in a high interference zone the data rates will drop sharply, in line with the Shannon capacity [9]. These low SNR operating conditions will degrade the user experience and expectations. One sensible way to solve this degradation is to use high gain beam-steering antennas. A high gain antenna increases a wireless device received power. Beam-steering would enable the device to navigate away from interferences and noise. Both together will push up the effective SNR and in turn the throughput [10]-[12].

In this paper, we demonstrate using a real-world example giving throughput values on how in weak SNR environment beam-steering antenna can make significant difference. We achieve this by designing and practically implementing a low cost high gain intelligent beam steering antenna system. We used off-the-shelf components to ensure compliance with future consumer wireless systems. We choose 2.45 GHz as the test frequency and OFDM WiFi as test protocol. This choice is underpinned with it being a high throughput mature technology from off-the-shelf perspective and it also scales gracefully to both higher and lower frequency spectrum.

For beam-steering antenna we selected single element four feeds based Square Loop Antenna (SLA). It is similar to [13]-[18], but is the first SLA developed on a hemispherical platform with a large substrate size. An important aspect of 5G would be high speed connected cars. We selected full hemispherical conformal shape to ensure that our system would easily adapt to various vehicular top and side platforms. In addition, the conformed shape is relevant for implementation in the future technologies (e.g. Internet of Things) in which wireless sensors platforms would be of random shapes. The antenna radiates four tilted beams having a gain of 8.9 dBi in a 90° azimuth space (single quadrant), one corresponding for each of the feeds. Using a Single Pole Four Throw (SP4T) RF switch [19] the antenna is capable of switching feeds sequentially one at a time and that it can steer a high gain beam in the full 360° azimuth space. Whilst we could have used phased arrays for beam-steering, that choice would had been expensive, lossy and importantly it would

A. Pal, A. Mehta and H. Goonesinghe are with College of Engineering, Swansea University, Swansea, SA28PP, U.K. (email: a.pal@swansea.ac.uk, a.mehta@swansea.ac.uk, 668590@swansea.ac.uk).

D. Mirshekar-Syahkal is with the Department of Computing Science and Electronic Engineering, Essex University, Colchester, Essex CO4 3SQ, U.K. (e-mail: dariush@essex.ac.uk).

H. Nakano is with the Science and Engineering Department, Hosei University, Koganei, Tokyo 184-8584, Japan (e-mail: hymat@hosei.ac.jp).

have required large space area for incorporating multiple antenna elements [20]-[23]. The intelligence for beam steering is realized using Raspberry Pi2 model B [24]. Pi provides control signals for the RF switch. A smart 'Electromagnetic sense, Analyze and Lock' algorithm is developed using C language which sits on the Pi. The algorithm enables the antenna to ensure that the communication link is always locked in the strongest RSS (Receive Signal Strength) direction. Commercially RSS values are available from the wireless receivers in form of RSS. Hence, RSS is chosen for link optimization. Using a compressed High Definition (HD) video internet networking we demonstrate the effectiveness of the pattern adaptive system in sustaining the uninterrupted quality video. We demonstrate that in that weak signal environment a high gain beam-steering is the difference between HD communication and no communication at all. We also present a throughput performance comparison between Omni-directional monopole antenna and HSLA based system in the presence of an external Interference Source (IS).

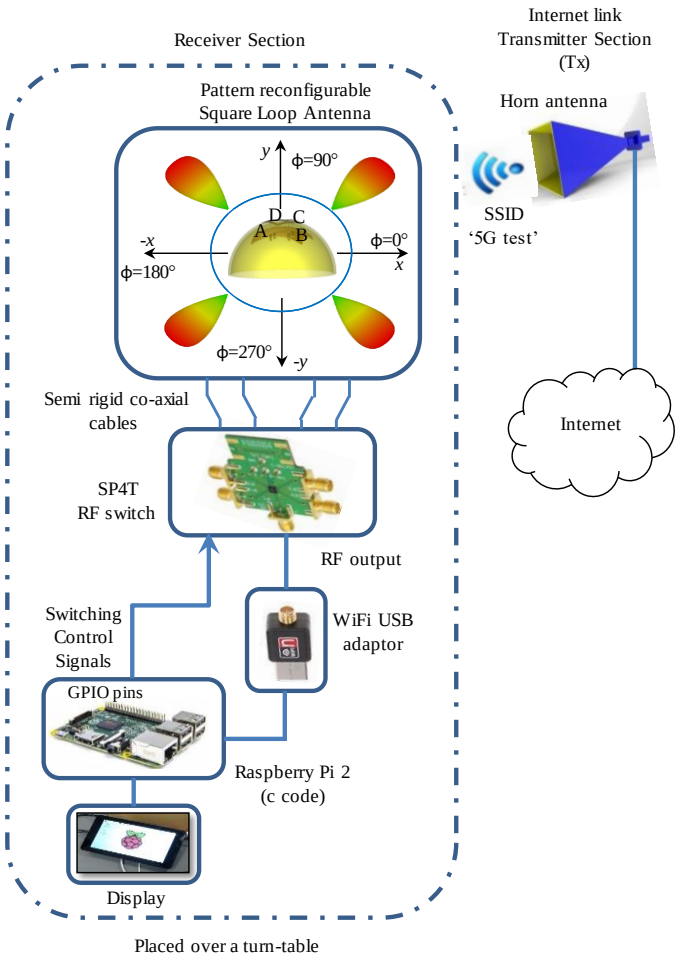

Fig. 1. Schematic of the beam-steering system.

II. Experimental Set-up

Fig. 1 shows the complete configuration of the implemented beam-steering system. The internet link Transmitter (Tx) is a horn antenna connected to the internet via a cisco router [25]. The horn antenna having a gain of 8.3 dBi provides a direct WiFi link to the receiver section and is placed on a wooden platform having a height of 70 cm, Fig 2. The Line of Sight (LOS) distance between Hemispherical Square Loop Antenna (HSLA) and horn is 1.3 meters in the far field region.

The receiver section consists of a conformal beam-steering HSLA combined with an SP4T RF switch and a single board computer - Raspberry Pi. The Pi unit is attached behind a 7-inch touchscreen display which is powered by a USB (Universal Synchronous Bus) battery (Fig. 2 (a)). The whole receiver section is placed on a turn table. For experimental purpose a near hemispherical Kevlar helmet is used as a substrate for the SLA.

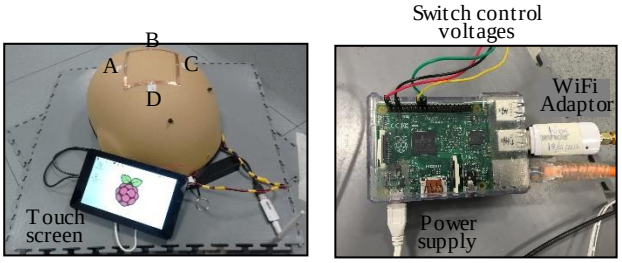

(a). HSLA and Raspberry Pi (b). Raspberry Pi

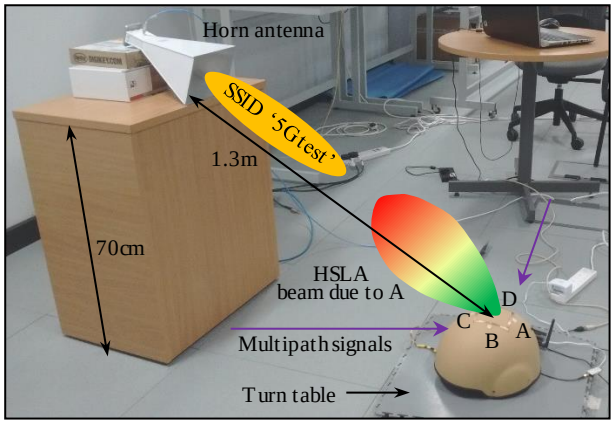

(c). Experimental set-up

Fig. 2. Experimental set-up including (a) HSLA, (b) Controller (Pi) and (c) Test environment.

The proposed system is designed to operate over 2.4 GHz (802.11b/g/n) WiFi band. Center frequency of this band (2.4 to 2.5 GHz) is 2.45 GHz and it is selected as the test frequency throughout this paper. Pi is provided the WiFi functionality using a USB based WiFi transceiver [26]. The Omni-directional monopole antenna for that transceiver is removed and the transceiver is directly connected to the SP4T RF switch. The switch then connects the transceiver to one of the four possible antenna ports. Based on which port is selected the antenna radiates a beam in one of the four possible spatial azimuth directions, as shown in Fig. 1. It should be noted that whilst it is a simple four quadrants beam steering architecture, it only covers azimuth beam steering. For achieving additional elevation steering a simultaneous multi-port excitation [27] can be considered.

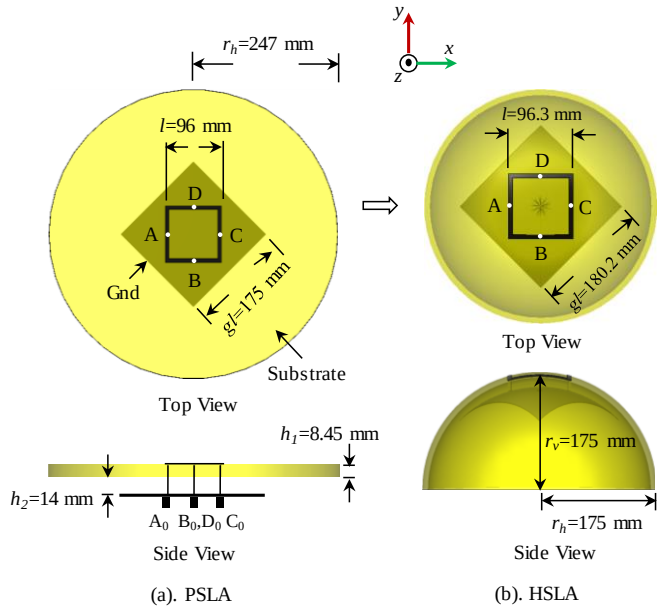

Fig. 3. Top and side views of the SLA. (a) The SLA on a planar substrate and (b) The SLA on a hemispherical substrate.

III. Hemispherical Square Loop Antenna (HSLA)

The previous work on beam steering square loop antennas [15]-[18] were on planar small size substrate platforms of length less than one wavelength. However, for the modern vehicles and sensor application the substrates are non-planar and have large sizes. To demonstrate beam steering on such conformal platforms we choose a hemisphere substrate of size over $4\lambda_0$ at the test frequency.

Fig. 3 shows the transition of Planar SLA (PSLA) to Hemispherical SLA (HSLA). Fig 3 (a) shows the top and side view of the PSLA on a circular substrate. The square loop is placed on top of a circular substrate having a radius of 247 mm (horizontal radius, r_h). The antenna substrate consists of a stack of two dielectric layers. The dielectric material Kevlar (ε_r =3.4) is used as top layer which has a height of h_1=8.45 mm. The bottom layer has a height h_2 =14 mm and is made of Rohacell 51 foam (ε_r =1.08). Hence, the total height of the antenna is 22.5 mm. This height and its two-layer configuration is selected as it is the height of the commercially available Kevlar Helmet (hemisphere substrate in this work). The radiating square loop is composed of four copper strips having a length l=96 mm and a track width w=5 mm. The loop is excited at four middle points (A, B, C and D) of the four arms by four vertical probes having a diameter of 1.3 mm. The probes are connected to the four standard SMA (*SubMiniature version A)* ports A_0, B_0, C_0 and D_0, respectively at the bottom of ground plane. The square shaped metallic (Copper) ground plane has an area of 175 mm×175 mm and it is rotated by 45° in the *xy*-plane with respect to the square loop. Fig. 3 (b) shows the PSLA conformed to HSLA. This is achieved by bending the PSLA from sides in which the middle portion of the ground plane along with substrate, feeds and square loop are raised. To keep the constant surface area, the bending causes reduction in horizontal radius r_h=175 mm, an increase in vertical radius r_v=175 mm, and a stretching of the ground plane (180.2 mm×180.2 mm). The length of each strips of square loop only increases by 0.3 mm in transition from the PSLA to HSLA.

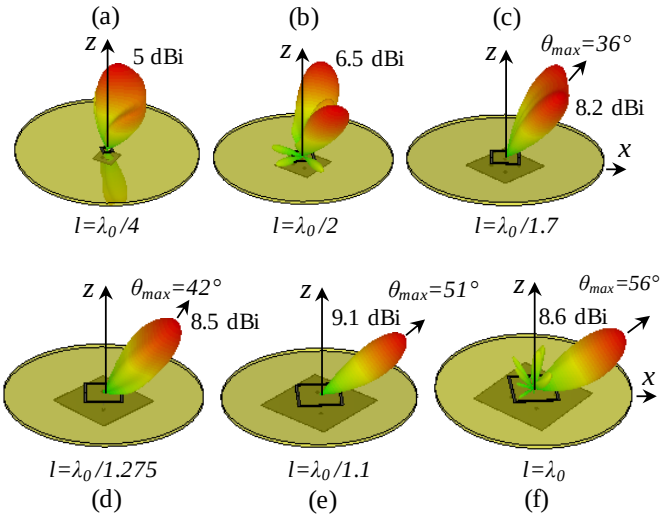

Fig. 4. Effect of different arm length (l) of square loop on radiation pattern at 2.45 GHz.

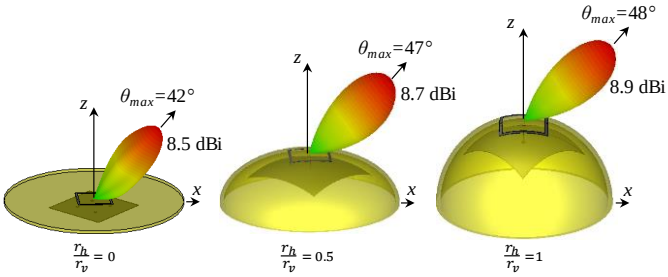

Fig. 5. Effect of substrate bending on the radiation pattern at 2.45 GHz.

Fig. 4 shows the design logic for the selection of the square arm length on a large substrate. It shows the effect of different arm lengths (l) of the square loop on the antenna radiation patterns at 2.45 GHz. In the simulations, the ratio of square loop arm length to the length of the ground plane (l/gl) is kept constant at 0.55. When only port A_0 is excited and the remaining ports (B_0, C_0 and D_0) are open-circuited the antenna main beam is a linearly polarized tilted beam (θ_{max}) directed away from the excited port A_0 (i.e. ϕ_{max}=0°).

For realizing a high throughput and mitigate multipath the aim is to achieve a tilted beam of a gain over 8 dBi with side lobes levels less than that of -7dB. It is found that for small arm lengths (Fig 4 a, b, c) the antenna patterns either had split beams or low gains. This is due to surface wave propagation in the large substrate. Further, it is found that only when the single arm loop length is kept between $\lambda_0/1.7 \leq l \leq \lambda_0/1.1$ the antenna provides a high gain titled beam with low side lobes. Therefore, l=96 mm (l= λ_0/1.275) is selected as the final dimension of the square loop. The track width (w) of the square loop is optimized to 5 mm for providing the highest antenna gain of 8.5 dBi with the widest impedance bandwidth.

Fig. 5 shows the effect of the substrate bending on the

antenna radiation patterns at 2.45 GHz when the ratio of r_h to r_v is varied. It is observed that when r_h/r_v is varied from 0 to 1 (Fig. 5), beam tilt angle varies from 42° to 48° and the gain increases from 8.5 dBi to 8.9 dBi. It is found that if the substrate is bent beyond r_h/r_v >1.3, magnitude of side lobe increases and pattern becomes distorted. The hemispherical configuration (r_h/r_v=1) of the antenna is selected due to the highest tilt angle and gain.

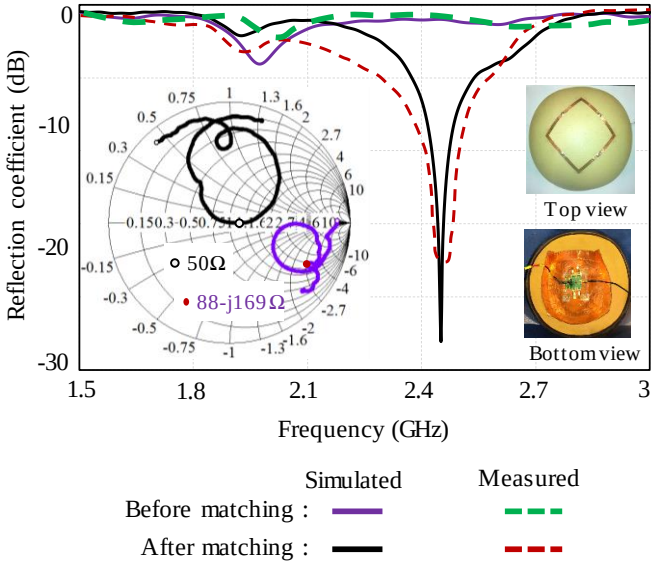

Fig. 6. Reflection coefficient and input impedance of the HSLA; (inset) top and bottom view of fabricated prototype.

Fig. 6 shows the frequency response of the reflection coefficient and input impedance of the HSLA. The antenna shows an input impedance of 88-j169Ω at the 2.45 GHz. This causes an impedance mismatch with the standard 50Ω excitation source. Consequently, the antenna exhibits a poor reflection coefficient ($|S_{11}|$ ~ -3dB) at the operating frequency. A two-section stepped coaxial transmission line matching circuits are employed to match the antenna to the switch.

Fig. 7 (a) and (b) show the simulated model and fabricated prototype of two-section stepped transmission line matching network. The matching network is developed using an FR4 substrate having permittivity of 4.8 and a height of 1.6 mm. The initial values of the characteristic impedance and length of the microstrip line are obtained from [28], and subsequently an optimizer of CST Microwave Studio (CST-MWS) [29] is used for achieving the final values. The matching network on the microstrip has two 9 mm long SMA standard connectors on its either sides. The matching network transforms 88-j169.3Ω from the input of HSLA to 50Ω. Fig. 6 also shows the reflection coefficient and input impedance of the HSLA when each port is connected to a matching network. With the matching networks, the HSLA operates efficiently ($|S_{11}|$ < -10 dB) over 2.4 GHz WiFi frequency band with an impedance bandwidth of 180 MHz (2.36 to 2.54 GHz).

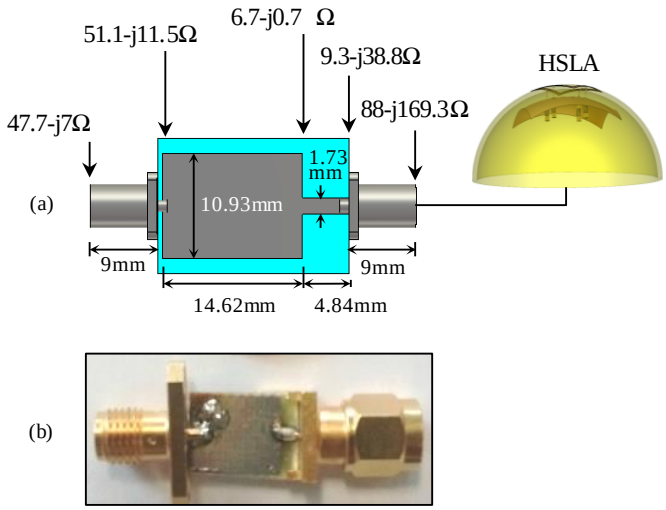

Fig. 7. Matching network: (a) Simulated model and (b) Fabricated prototype.

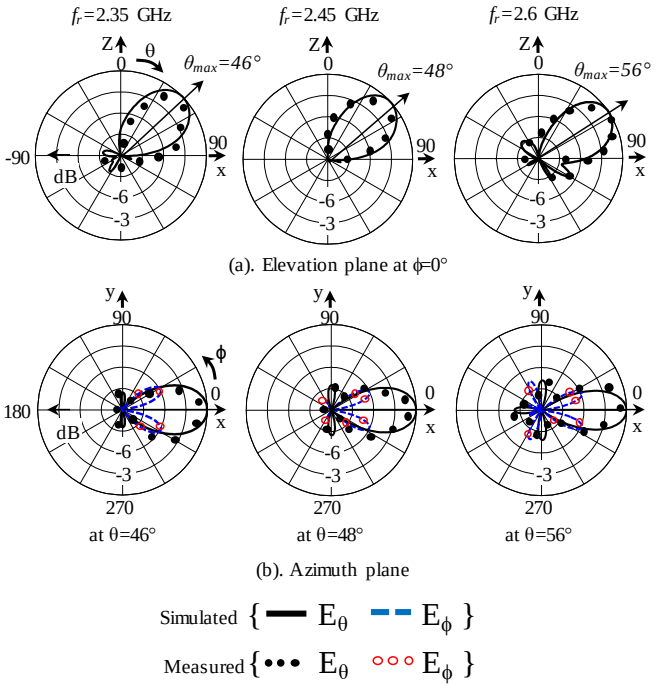

Fig. 8. Radiation patterns of the HSLA over the operating bandwidth. (a) Elevation cut is at ϕ = 0. (b). Azimuth cut is at θ= 46°, 48° and 56° for 2.35, 2.45 and 2.6 GHz, respectively.

When port A_0 is excited and the remaining ports (B_0, C_0 and D_0) are open circuited, the HSLA provides a linearly polarized beam, tilted at θ_{max}=48° from the zenith (z-axis). The beam is pointed away from the excited port, i.e. in the direction of ϕ_{max}=0°. With the matching network, the HSLA provides a gain of 8.9 dBi in the direction of maximum radiation with a radiation efficiency greater than 87% over the impedance bandwidth. The main radiation beam is linearly polarized (E_θ) in the direction of maximum radiation. In the elevation cut the magnitude of the cross-polarized (E_ϕ) component is well below that of the co-polarized component (E_θ), i.e. $|E_\theta|>|E_\phi|$ by over 40 dB. Hence not visible in the Fig. 8. In the azimuth cut the magnitude of E_ϕ is 6 dB down from E_θ, however it is

not in the main lobe direction. It is shown in Fig. 8 that the SLA maintains its pattern shape over the radiation pattern bandwidth of 250 MHz (2.35 to 2.6 GHz). A variation of 10° (46° to 56°) in beam tilt angle and a variation 0.5 dB (8.5 to 8.9 dBi) in gain are observed over the radiation pattern bandwidth. Outside the pattern bandwidth, the radiation patterns are distorted due to split beam.

Since the square loop is symmetrical with respect to the centre point of the whole structure, the radiation patterns of other feeding ports (B_0, C_0 and D_0) are similar to that of port A_0. Therefore, when any of the four feeding ports are excited one at a time, while the remaining ports are open circuited, the HSLA provides a tilted beam of θ_{max}=48° in four different space quadrants of ϕ_{max}=0°, ϕ_{max}=90°, ϕ_{max}=180° and ϕ_{max}=270°. Thus, by switching the RF input along the feeding ports the HSLA maneuvers its radiation beam over the four quadrants to scan the entire 360° space in front of the antenna. We achieve this beam steering by using an RF switch and an intelligent algorithm for RSS enhancements. However, if the operational scenarios include a presence of jamming / interference then SINR / throughputs should be chosen as enhancement criterions. It is described in the next section.

IV. Throughput Analysis

As shown in Fig. 1, the SP4T RF switch is connected to the HSLA using four semi-rigid coaxial cables, each having a length of 110 mm. The RF Output of the switch is connected to the USB WiFi adapter (transceiver) which is interfaced with Raspberry Pi where throughput is measured and examined. The control pins of the RF switch are connected to the GPIO (General-purpose input/output**)** pins of the Raspberry Pi that provide the necessary required biasing and switching control voltages. Raspberry Pi runs an intelligent beam-steering algorithm written in C called 'Electromagnetic Sense, Analyze and Lock' algorithm. It enables HSLA to lock always to a direction along which the Pi receives the strongest RSS signal value. This algorithm is shown in Fig. 9.

In Fig. 2, laboratory set up, upon powering of the system the RF switch undertakes a fast-sequential switch / scan (in 100 milli sec) of the environment. This provides the four RSS values for the signal received at the four HSLA ports from the WiFi channel being transmitted from the horn antenna. The horn antenna is set to transmit vertical polarization (E_θ) WiFi signals at SSID (Service Set Identifier) '5G test' which is synchronized with the WiFi transceiver chip. The Pi compares the four RSS values and locks the system to the port with highest value. Table 1 shows the four received RSSs for the four ports and that the system is auto locked to the strongest RSS port A_0 (-65 dBm). Thereafter, the system keeps monitoring the link. We set a dynamic setting to ensure that whenever a signal drops below a threshold level the system undertakes a fresh scan. For this work, we have a setting that 'if signal drops 3 dB below the current RSS, in this instance -68 dBm' it undertakes a new scan. The threshold to rescan is dynamic and by using a slider on Graphic User Interface on the display it can be changed easily for any desired value. Both Tx and HSLA are moved around the laboratory and it is found that in all instances the algorithm always locked to the strongest RSS signal direction.

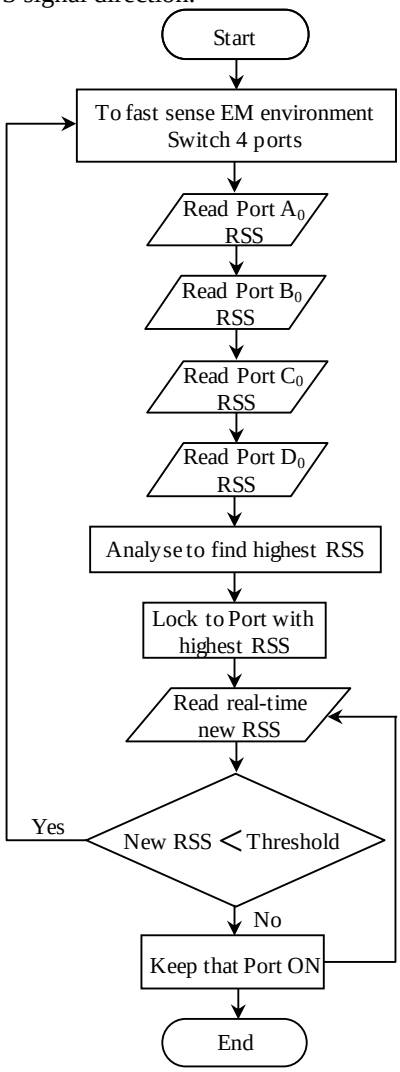

Fig. 9. Flowchart of the Electromagnetic sense, Analyse and Lock algorithm.

We tested the system internet throughput on all four ports and found that there was a significant difference between the strongest and weakest signal ports. For instance, the strongest port A_0 provided an RSS of -65 dBm, a downlink of 6.1 Mbps (Megabits per second) and an upload speed of 4.3 Mbps. This meant that port A_0 can fully support compressed HD duplex video link. In contrast, internet throughput measurements on other weaker ports (B_0, C_0 and D_0) which are operating close to the system average noise floor in multipath laboratory setting of -81 dBm provides extremely weak data rates; even down to zero kbps for both upload and download speeds. This value of noise floor for the WiFi receiver chip is the lowest value below which the internet link breaks and receiver needs restarting. For instance, port D_0 RSS is just 2 dB above noise floor and provides zero data speeds with the commercial WiFi modulation schemes. Therefore, the beam steering enhances the throughput and its capacity for the fixed available WiFi bandwidth. These tests are done on a commercial throughput-measuring web-site. In addition, the internet horn antenna link is not shared with any other user and is totally dedicated to

this experiment. This test quantifies the beam steering advantage in a real world of OFDM communications (which will also be the basis of 5G systems). It shows that a high gain beam steering antenna enables a device to lock to the direct / strongest signal, and that the device could sustain compressed HD video in an otherwise weak SNR environment. Had the beam steering not present in the same environment, in a worst case scenario the same device would have absolutely zero throughput. This advantage is further evident from the video test that is undertaken. It shows that a compressed HD is sustained by port A_0 with zero packet and frame loss. The other ports offer video conferencing with a weak intermittent service with 90 % packet loss or absolutely no service at all. Thus, for a given weak EM environment beam steering is the difference between a good HD communication versus a very weak or no communication.

Table. I. RSS, throughput and video qualities of the communication link '5G test' at four ports of the HSLA.

		Port A_0	Port B_0	Port C_0	Port D_0
RSS for '5G test' (dBm - average of five repetitions)		**-65 (locked)**	-75	-77	-79
Throughput (Mbps)	Download	**6.1**	0.9	0.3	0
	Upload	**4.3**	0.7	0.3	0
highest Packet Loss observed (%)	Send	**0**	90	96	98.1
	Receive	**0**	90	92.4	97
Video Conference link ON/OFF?		**ON**	Intermittent breaking	OFF	OFF

We are using only a single antenna for both sensing and communication. Typically, besides a communication antenna an additional auxiliary antenna is needed for electromagnetic environment sensing. We did not need a sperate sensing antenna as we exploited the built-in buffers and latency mitigation mechanisms of the TCP / IP WiFi network. These buffers ensured that no data is lost in the 100 milli second scan / sense duration. Note, while the switches can operate in nano seconds, a milli seconds scan duration is selected due to relatively slow time response of the USB WiFi adapter. Although, this work is based on RSS, if an actual jamming / interference occurs it will contribute to increase RSS but dropping of the throughput. Thus, in such scenarios the switching logic would need to be implemented on SINR instead of RSS.

Finally, as demonstrated in this work the algorithm works at the application layer that controls the RF switch and antenna patterns at physical layer. Therefore, in this work the entire middle protocol layers are untouched. Hence, the system can easily be retrofitted to existing non-adaptive communication systems to make them smarter and faster in weak EM environments.

V. Performance Analysis of HSLA in Comparison with Conventional Omni-directional Monopole Antenna

In this section, a performance comparison of the system (Fig. 1) is done between omni-directional monopole antenna (typical gain of 3 dBi) and the HSLA (gain of 8.9 dBi). The results presented are based on the field measurements in various indoor environments in the presence of an Interference Source (IS). In total three indoor environments are investigated which are described next.

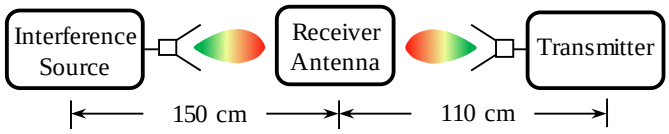

Fig. 10. Schematic of LOS transmitter and LOS interference source configuration for a short distance.

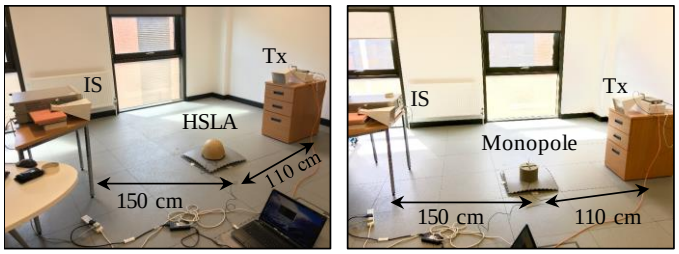

Fig. 11. Experimental set-up for throughput measurement in LOS (Line of Sight) transmitter and LOS interference source configuration for a short distance. (a) HSLA based system and (b) Omni-directional monopole antenna based system.

A. LOS transmitter and LOS interference source configuration for short distance

Fig. 10 shows the schematic of the LOS (Line of Sight) internet link Transmitter (Tx) and LOS Interface Source (IS) for a short distance. The Tx horn antenna is placed at a distance 110 cm away from the receiver antenna and transmit power is set to -27 dBm. The IS horn antenna is placed directly opposite to the Tx at distance 150 cm away from the receiver. The receiver antenna is positioned in the middle. The Tx and IS horn antennas are pointed to the receiver antenna to ensure the LOS propagation. Fig 11 shows the experimental set up. It is observed that when the IS is switched off ('off') the HSLA and omni-directional monopole antenna based system provides a throughput of 6.1 Mbps and 4.3 Mbps, respectively as shown in Fig. 12. This and all throughput numbers in this section are an average of 5 repeated readings. Thus, HSLA based system offers 42% higher throughput due to the higher gain of 8.9 dBi compared to the monopole antenna gain of 3 dBi. However, when the magnitude of the interference increases the HSLA provides more superior performance compared to the monopole antenna. The HSLA based system provides a higher throughput by 90% and 1225% when the interference magnitude are 0 dBm and 5 dBm, respectively. When the interference magnitude increases beyond 5 dBm the communication link of the monopole antenna based system completely breaks down. However, the HSLA based system can sustain the link of 1.4 Mbps even up to 15 dBm of interference (a graceful and gradual reduction).

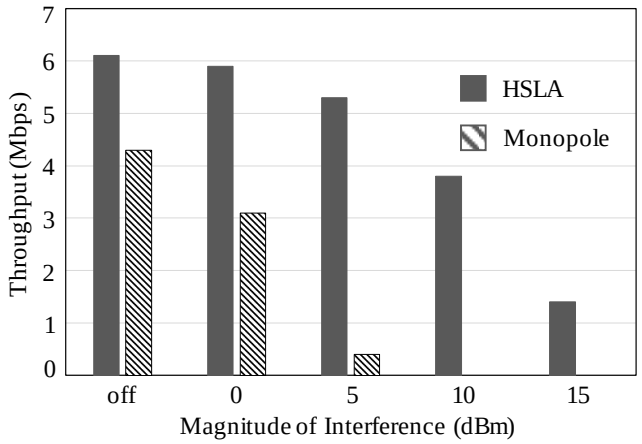

Fig. 12. Throughput (average of 5 reading) of HSLA and Omni-directional monopole antenna based system in LOS transmitter and LOS interference source configuration for a short distance (Fig. 10).

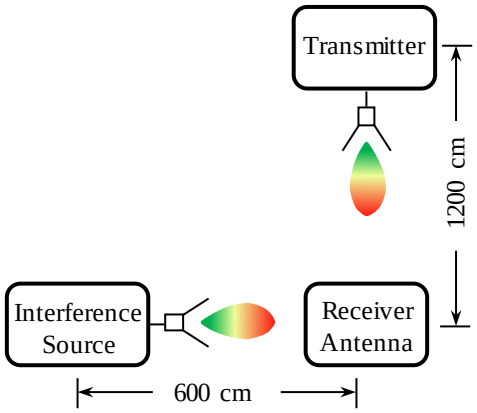

Fig. 13. Schematic of LOS transmitter and LOS interference source configuration for a long distance.

B. LOS transmitter and LOS interference source configuration for a long distance

We also compared the performances of LOS Tx and LOS IS configuration for a long distance. In this case the Tx is placed at 1200 cm away from the receiver and the Tx power is increased by 10 dB and set to -17 dBm. The IS is positioned at distance of 600 cm from the receiver and is placed orthogonally left of the receiver as shown in Fig. 13. Due to the complex reflective EM environment of the laboratory this configuration enables a creation of a rich multipath scattering setting. This severely affects the performance of the monopole antenna based system. Even with the interference 'off' its average throughput drops to 0.3 Mbps (Fig. 14). However, the HSLA based system provides the communication link with an average throughput of 3.5 Mbps. Further, when interference magnitude is set between 0 dBm and 10 dBm the HSLA through put is more than 10 times compared to that of the monopole antenna as shown in Fig. 14. Beyond 10 dBm of interference the communication link of the monopole antenna based system completely breaks down. The HSLA based system continues to work with interference up to 15 dBm power. Hence, this shows that in the scattered environment the HSLA not only offers a much higher throughput but also can sustain a higher interference compared to a monopole based static system.

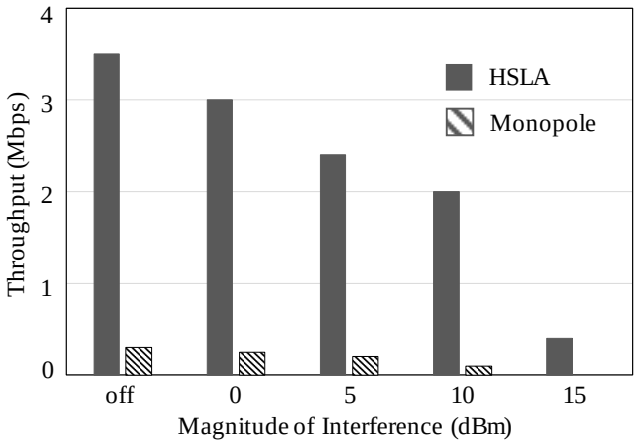

Fig. 14. Average throughput of HSLA and Omni-directional monopole antenna based system for configuration shown in Fig. 13.

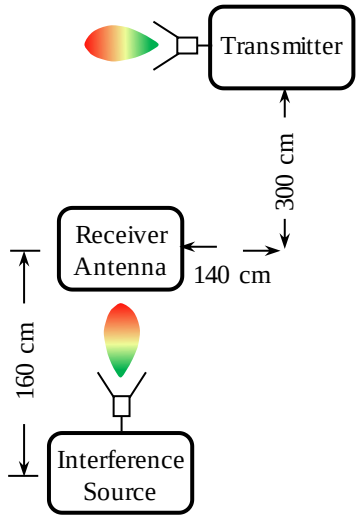

Fig. 15. Schematic of Non-Line Of Sight (NLOS) transmitter and LOS interference source configuration.

C. Non-Line of Sight (NLOS) transmitter and LOS interference source configuration

We also compared the performance of the HSLA and monopole antenna when the Tx is in Non-Line of Sight (NLOS) and IS is in LOS configuration as shown in Fig. 15. The Tx power in this case is set to +5 dBm. Fig. 16 shows the comparison of the measured throughputs for different level of interferences. When the IS is off, the HSLA based system provides approximately 53% better throughput compared to the monopole antenna based system. It is observed that when the interference magnitude increases from 0 dBm to 20 dBm the increment in average throughput of HSLA based system over the monopole based system also increases from 76% to 1450%, respectively. The communication link of monopole antenna breaks down beyond interference magnitude of 20 dBm. However, the HSLA based system maintains the communication link of an average throughput of 3.1 Mbps even with the interference magnitude of 25 dBm.

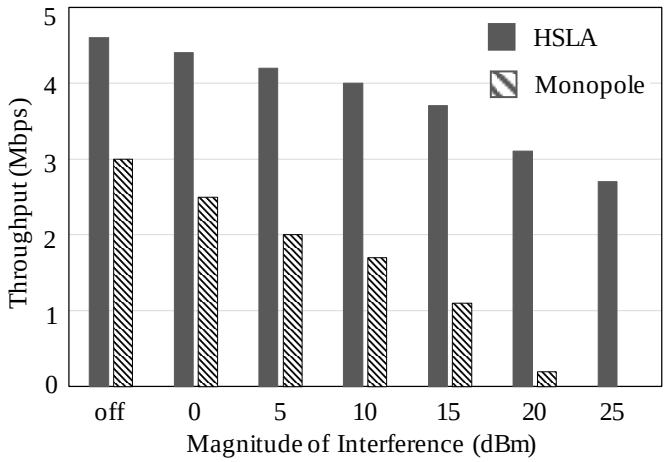

Fig. 16. Average throughput of HSLA and Omni-directional monopole antenna based system for configuration shown in Fig. 15.

VI. Conclusion

A pattern adaptive Hemispherical Square Loop Antenna (HSLA) is controlled by Raspberry Pi single board computer. It is demonstrated that in a weak EM environment the adaptive antenna is capable of providing a throughput 6.1 Mbps and can sustain uninterrupted compressed HD video conference. It is also demonstrated that in the absence of beam steering capability there will be practically no communication (0 bps). The beam steering mechanism is implemented using a smart 'EM Sense, scan, analyze and lock' algorithm running on Pi in C. The algorithm controls the beam direction of the SLA by using an RF SP4T switch linked to the SLA. The proposed system architecture uses only a single antenna for both sensing and communications. Finally, the system has the application layer controlling the physical layer for a maximum possible RSS. Thus, the entire middle protocol layers are untouched. Three different indoor internet received configurations were investigated in presence of interference. It is demonstrated that the HSLA based system provides can provide more than 1450 % higher average throughput compared to the conventional Omni-directional monopole antenna based system.

References

[1] Cisco, "Cisco Visual Networking Index: Global Mobile Data Traffic Forecast Update 2014–2019" White Paper, 2015.

[2] A. Aloman, A. I. Ispas, P. Ciotirnae, R. Sanchez-Iborra and M. D. Cano, "Performance Evaluation of Video Streaming Using MPEG DASH, RTSP, and RTMP in Mobile Networks," *IFIP Wireless and Mobile Networking Conference (WMNC)*, Munich, 2015, pp. 144-151.

[3] E. Yaacoub, Z. Dawy, and A. Abu-Dayya, "On real-time video streaming over lte networks with mobile-to-mobile cooperation," *International Conference on Telecommunications (ICT), IEEE*, 2012, pp. 1–6.

[4] "MobiTV", [Online]. Available: https://www.mobitv.com/.

[5] R. Anderson, O. Chung, K.M. Davis, P. Davis, C. Prince, V. Razmov, and B. Simon, "Classroom presenter—a classroom interaction system for active and collaborative learning," *Proc. Workshop Impact of Pen-Based Technology on Education (WIPTE)*, 2006.

[6] "Smarthome-Home Automation Systems, Products, Kits, Hubs & Ideas", [Online]. Available: http://www.smarthome.com/.

[7] W. Coomans *et al*., "XG-fast: the 5th generation broadband," *IEEE Commun. Mag.*, vol. 53, no. 12, pp. 83-88, Dec. 2015.

[8] C.-X. Wang et al., "Cellular Architecture and Key Technologies for 5G Wireless Communication Networks," *IEEE Commun. Mag*., vol. 52, no. 2, pp. 122–30, Feb. 2014.

[9] C. E. Shannon, "Communication in the Presence of Noise," *Proc. I.R.E*, vol. 37, no. 1, pp. 10-21, Jan. 1949.

[10] R. R. Choudhury, Xue Yang, R. Ramanathan and N. H. Vaidya, "On designing MAC protocols for wireless networks using directional antennas," *IEEE Trans. Mobile Computing*, vol. 5, no. 5, pp. 477-491, May 2006.

[11] V. Navda , A. P. Subramanian , K. Dhanasekaran , A. Timm-Giel and S. Das, "MobiSteer: using steerable beam directional antenna for vehicular network access," *Proc. 5th international conference on Mobile systems, applications and services*, San Juan, Puerto Rico, Jun. 11-13, 2007.

[12] X. Liu, A. Sheth, M. Kaminsky, K. Papagiannak, S. Seshan, and P. Steenkiste, "DIRC: Increasing indoor wireless capacity using directional antennas," *Proc. ACM SIGCOMM*, Aug. 2009, pp. 171–182.

[13] A. Mehta, D. Mirshekar-Syahkal, and H. Nakano, "Beam adaptive single arm rectangular spiral antenna with switches," *IEE Proc. Microwave, Antennas Propag.*, vol. 153, no. 1, pp. 13–18, 2006.

[14] A. Pal, A. Mehta, D. Mirshekar-Syahkal and P. J. Massey, "Doughnut and tilted beam generation using a single printed star antenna," *IEEE Trans. Antennas Propag.* , vol. 57, no. 10, pp: 3413-3418, Oct. 2009.

[15] A. Mehta and D. Mirshekar-Syahkal, "Pattern steerable square loop antenna," *IEEE Electron. Lett.*, pp. 491–493, Apr. 2007.

[16] A. Pal, A. Mehta, D. Mirshekar-Syahkal, and P. J. Massey, "Short circuited feed terminations on beam steering square loop antennas," *IEEE Electron. Lett.*, vol. 44, no. 24, pp. 1389–1390, Nov. 2008.

[17] P. Deo, A. Mehta, D. Mirshekar-Syahkal, P. J. Massey and H. Nakano, "Thickness reduction and performance enhancement of steerable square loop antenna using hybrid high impedance surface," *IEEE Trans. Antennas Propag.*, vol. 58, no. 5. pp. 1477–1485, May, 2010.

[18] A. Pal, A. Mehta, D. Mirshekar-Syahkal, P. Deo, H. Nakano, "Dual-Band Low-Profile Capacitively Coupled Beam-Steerable Square-Loop Antenna," *IEEE Trans. Antennas Propag.*, vol.62, no.3, pp.1204-1211, Mar. 2014.

[19] [Online].Available:https://www.hittite.com/content/documents/data_sheet/hmc241lp3.pdf.

[20] J. C. Wu, C. C. Chang, T. Y. Chin, S. Y. Huang and S. F Chang, "Sidelobe level reduction in wide-angle scanning array system using pattern-reconfigurable antennas," *Microwave Symposium Digest (MTT), 2010 IEEE MTT-S International*, Anaheim, CA, 2010.

[21] M. P. Daly and J. T. Bernhard, "Beam steering in Pattern Reconfigurable Arrays Using Directional Modulation," *IEEE Trans. Antennas and Propag.*, vol. 58, no. 7, pp. 2259-2265, Jul 2010.

[22] Y. Y. Bai, S. Xiao, M. C. Tang, Z. F. Ding and B. Z. Wang, "Wide-Angle Scanning Phased Array With Pattern Reconfigurable Elements," *IEEE Trans. Antennas and Propag.*, vol. 59, no. 11, pp. 4071-4076, Nov 2011.

[23] A. Pal, A. Mehta, R. Lewis and N. Clow, "Reconfigurable phased array antenna enabling a high gain wide angle beam scanning," *2015 IEEE International Symposium on Antennas and Propagation & USNC/URSI National Radio Science Meeting*, Vancouver, BC, 2015.

[24] Various, "Raspberry Pi model B credit card sized minicomputer," Raspberry Pi Foundation, UK, [online] http://www.raspberrypi.org/products/model-b/.

[25] http://www.cisco.com/c/en/us/products/collateral/wireless/aironet-1200-access-point/product_data_sheet09186a00800937a6.html.

[26] "Tenda U1 300Mbps Utral-Fast Wireless USB Adapter-Tenda-All For Better NetWorking," [Online]. Available: http://www.tendacn.com/en/product/U1.html.

[27] A. Pal, A. Mehta, D. Mirshekar-Syahkal and H. Nakano, "A Twelve-Beam Steering Low-Profile Patch Antenna With Shorting Vias for Vehicular Applications," *IEEE Trans. Antennas Propaga.*, vol. 65, no. 8, pp. 3905-3912, Aug. 2017.

[28] S. Rosloniec, "Design of stepped transmission line matching circuits by optimization methods," *IEEE Trans. Microwave Theory and Techniques*, vol. 42, no. 12, pp. 2255-2260, Dec 1994.

[29] CST GmbH. Darmstadt, Germany, [*online*] http://www.cst.com.